Asymmetric Magnetic Reconnection in the Solar Atmosphere

Nick Murphy

Harvard-Smithsonian Center for Astrophysics

Pre-Hurricane NIMROD Team Meeting
Providence, Rhode Island
October 27, 2012

Collaborators: Mari Paz Miralles, John Raymond, Drake Ranquist, Crystal Pope, Kathy Reeves, Chengcai Shen, Jun Lin, Trae Winter, Dan Seaton, Aad van Ballegooijen, Clare Parnell, Andrew Haynes, Lijia Guo, & Yi-Min Huang

SDO/AIA takes 4096^2 observations of the Sun in eight EUV wavelengths with a 12 second cadence

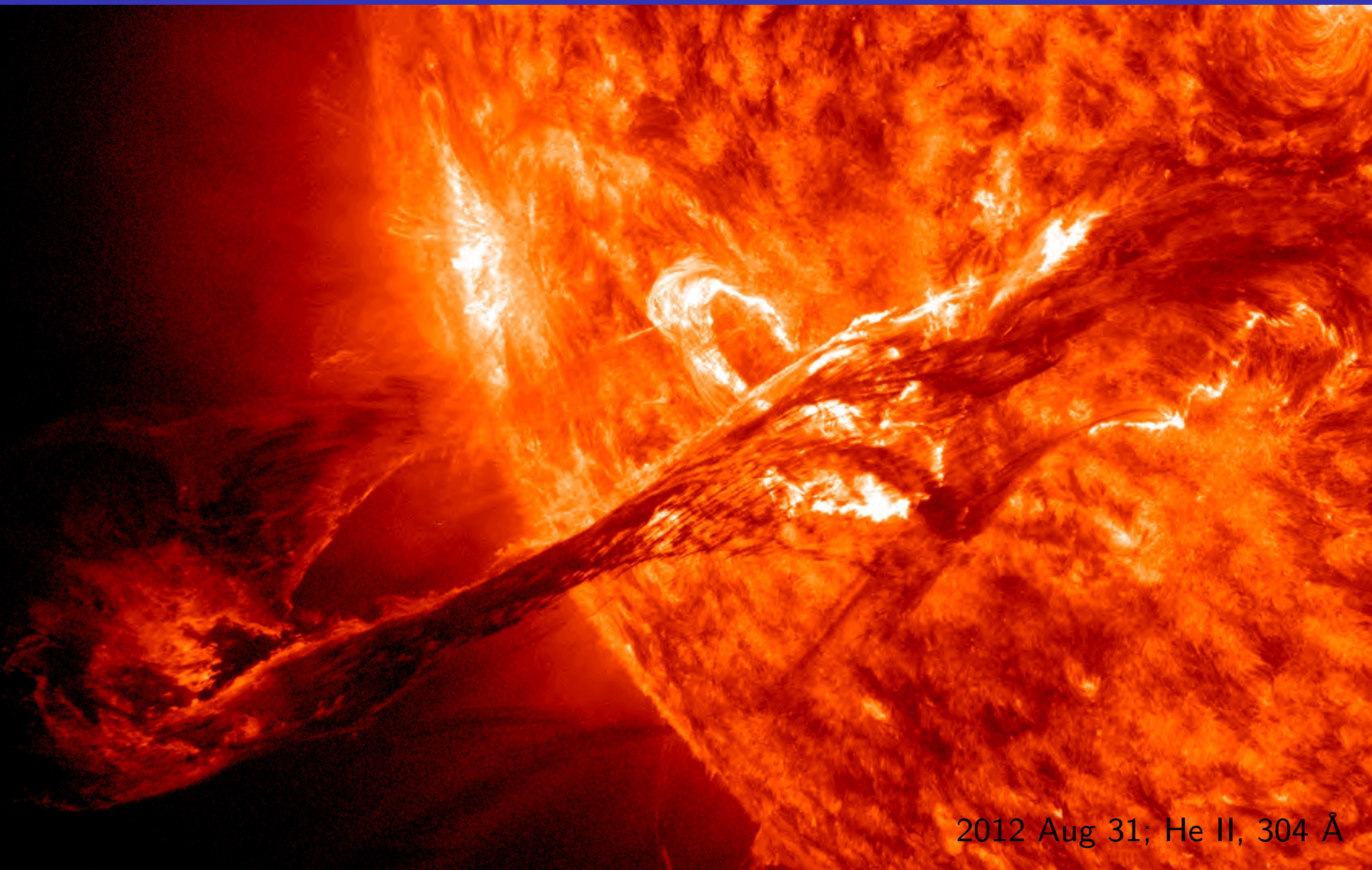

Overall science goal: To understand the dynamics and consequences of reconnection in the solar atmosphere

- NIMROD simulations of asymmetric reconnection (this talk)
- Analytic theory on appearance, disappearance, and motion of magnetic nulls (one slide)
- Non-equilibrium ionization modeling of coronal mass ejections (Murphy et al. 2011)
  - Ionization/recombination timescales are comparable to expansion time scales
  - Charge state distribution contains temperature history information
  - Evidence of significant heating, but mechanism(s) unclear
- Reconnection in partially ionized chromospheric plasmas
  - New collaboration with V. Lukin & J. Leake using HiFi code
  - Topics: inflow asymmetry, elemental fractionation, Hall effect
- Solar observations of reconnection (including asymmetry)

Introduction

- Most models of reconnection assume symmetry
- *Asymmetric inflow reconnection* occurs when the upstream magnetic fields and/or plasma parameters differ
  - Dayside magnetopause
  - Tearing in tokamaks, RFPs, and other confined plasmas
  - Merging of unequal flux ropes
  - 'Pull' reconnection in MRX
- *Asymmetric outflow reconnection* occurs, for example, when outflow in one direction is impeded
  - Flare/CME current sheets
  - Planetary magnetotails
  - Spheromak merging
  - 'Push' reconnection in MRX
- This talk covers
  - Reconnection with both asymmetric inflow and outflow
  - The plasmoid instability during asymmetric inflow reconnection

Flux rope models of CMEs predict a current sheet behind the rising flux rope

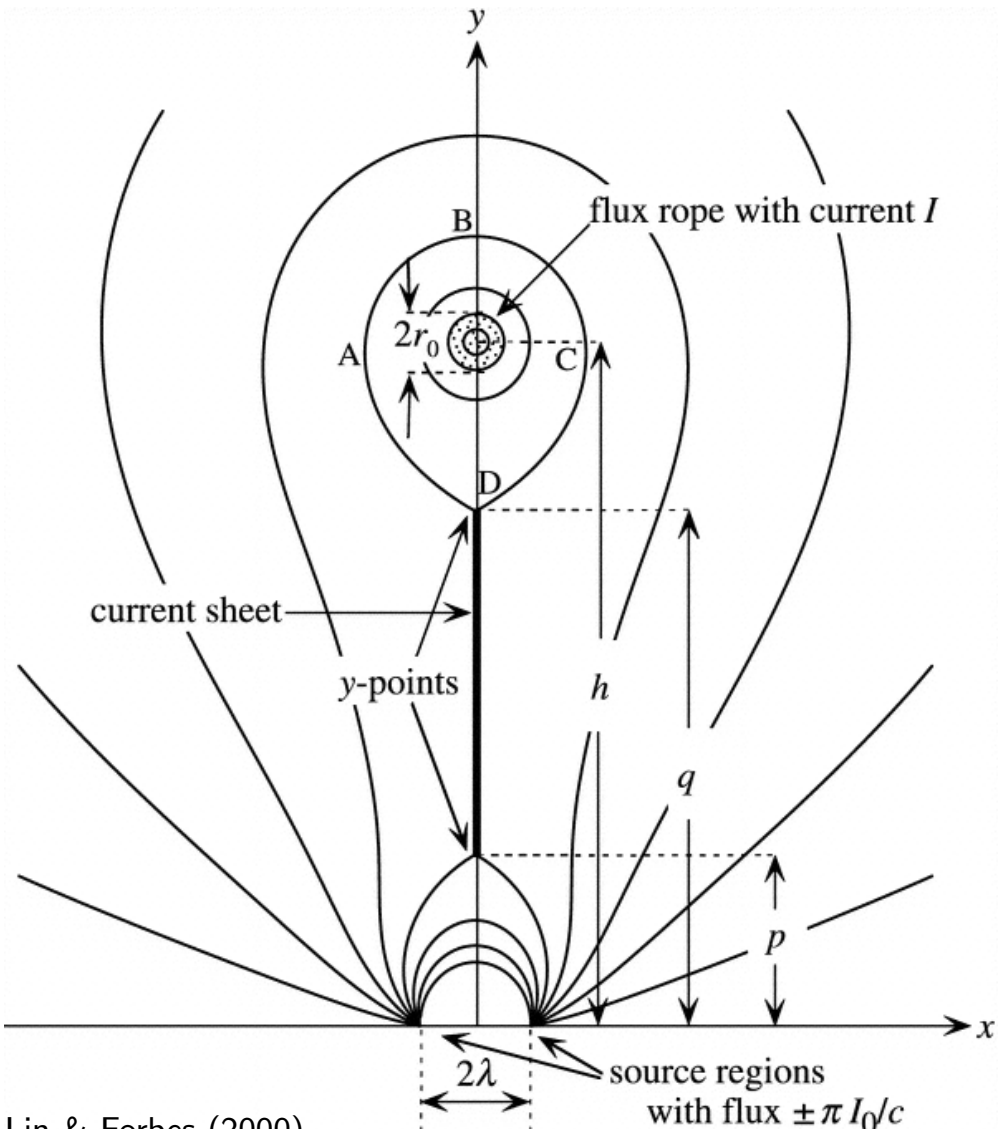

Lin & Forbes (2000)
'CSHKP' model

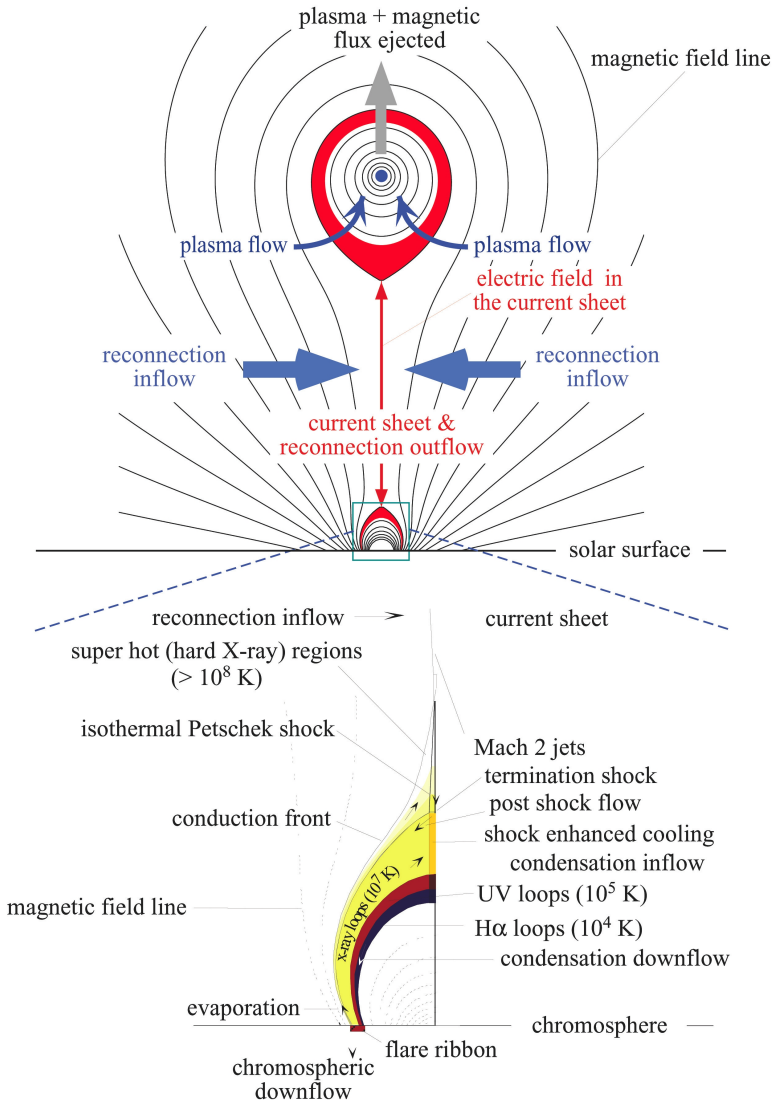

Signatures of reconnection: 'current sheet' structures

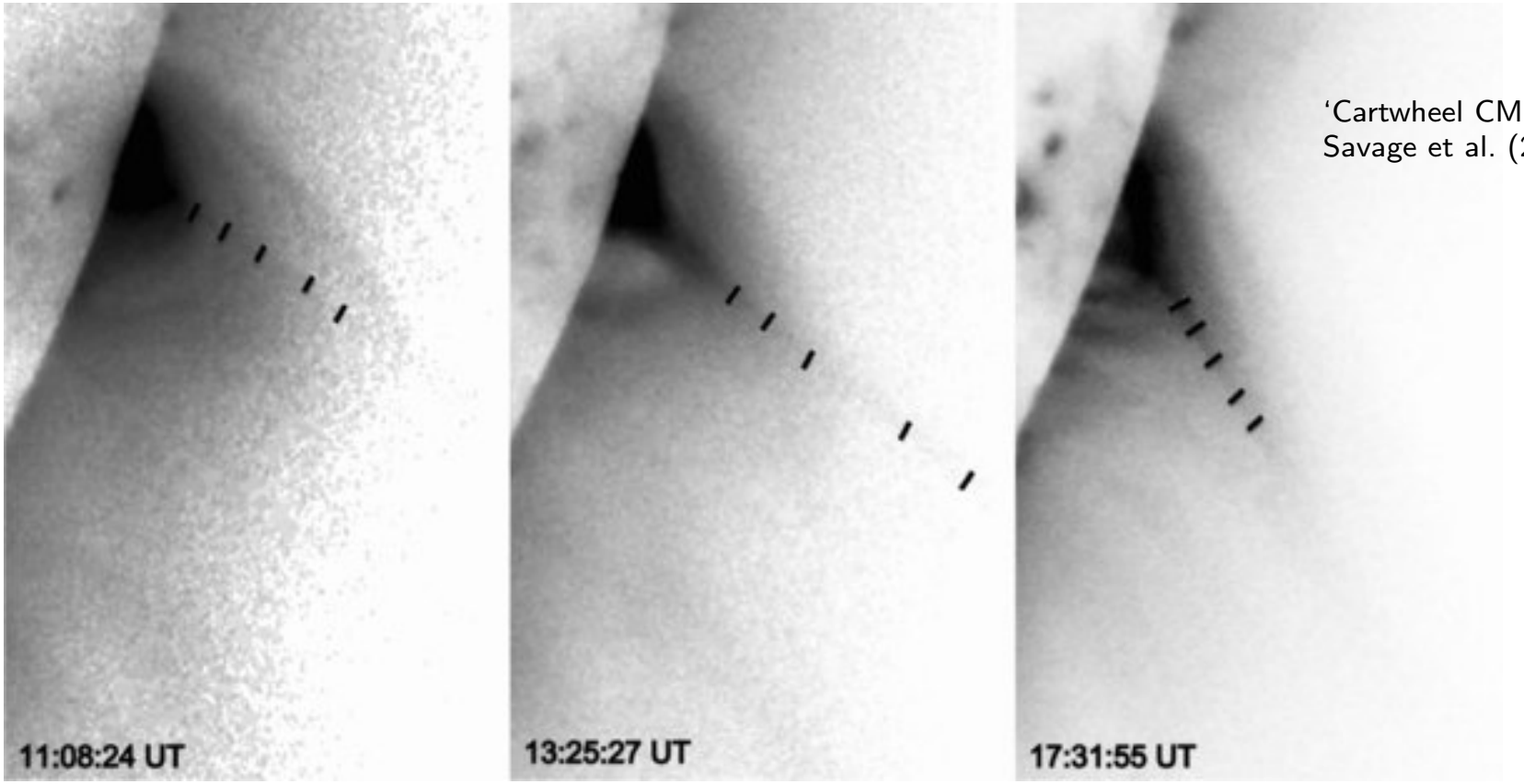

'Cartwheel CME'
Savage et al. (2012)

- White light, X-ray, and EUV observations show sheet-like structures between the post-flare loops and the rising flux rope
- Much thicker than expected; the current sheets may be embedded in a larger-scale plasma sheet
- Current sheets often drift considerably $\longrightarrow$ asymmetry?

Signatures of reconnection: inflows, upflows, downflows

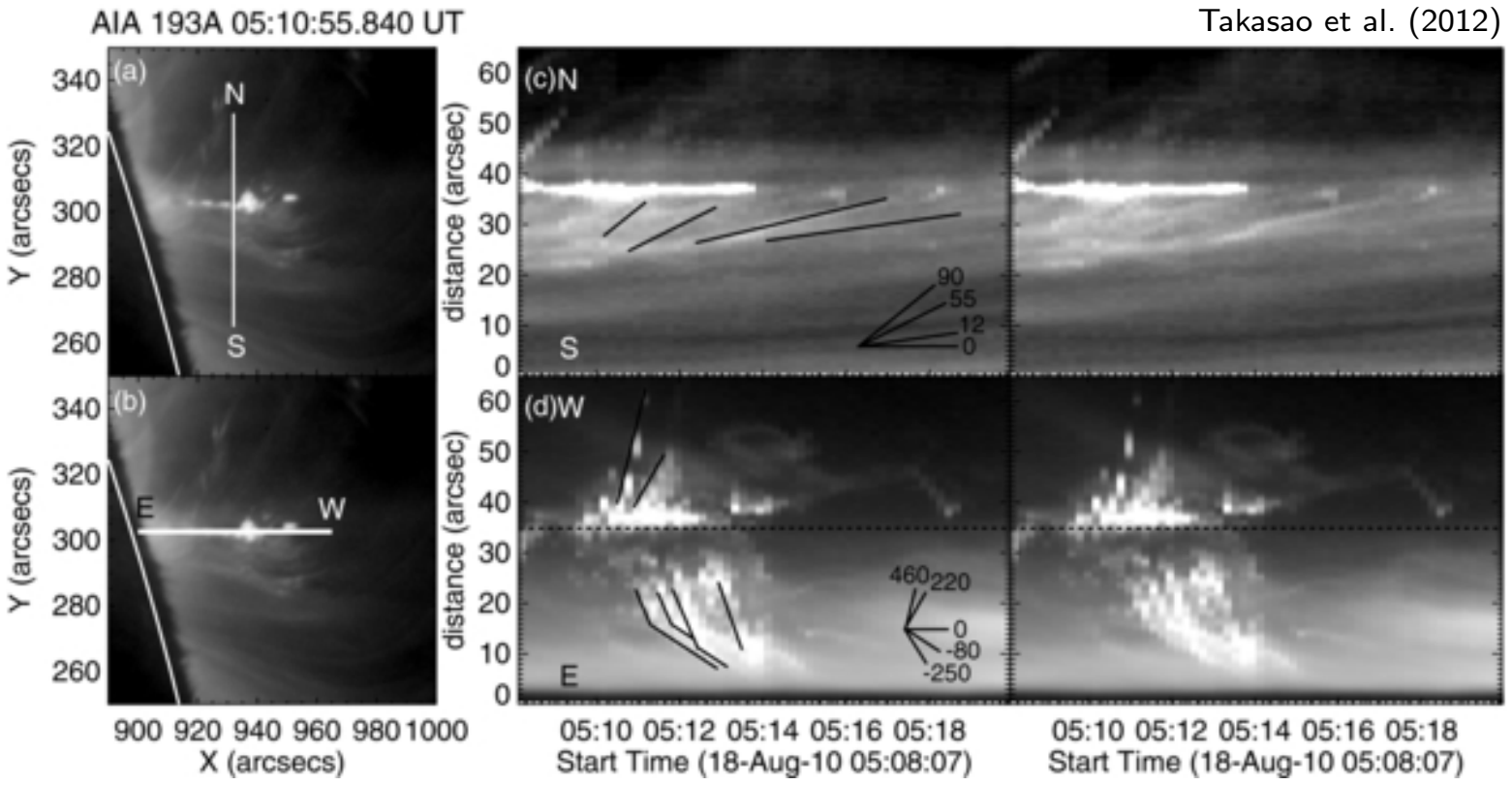

- High cadence observations show reconnection inflows and sunward/anti-sunward exhaust
- Supra-arcade downflows (SADs) re-interpreted as wakes behind contracting loops (Savage et al. 2012)
- Downflows often sub-Alfvénic: due to asymmetry? (Reeves et al. 2010; Murphy 2010; Murphy et al. 2010, 2012)

Open questions in solar/astrophysical reconnection

- What sets the reconnection rate?
- What are the small-scale physics of reconnection?
- What is the interplay between small and and large scales?
- Why is there a sudden onset to fast magnetic reconnection?
- Is the 3D plasmoid instability enough for fast reconnection, or are collisionless effects required?
- How are particles accelerated and heated?
- What sets the observed thickness of current sheets?
- How does 3D reconnection occur?
- What are the roles of turbulence, instabilities, and asymmetry?
- How does magnetic reconnection occur in partially ionized plasmas such as the chromosphere?

Part I: Line-tied asymmetric reconnection in the solar atmosphere

NIMROD simulations of line-tied asymmetric reconnection

- Reconnecting magnetic fields are asymmetric:

$$B_y(x) = \frac{B_0}{1+b} \tanh\left(\frac{x}{\delta_0} - b\right) \tag{1}$$

- Initial X-line located at $(x, y) = (0, 1)$ near lower wall
- Magnetic field ratios: 1.0, 0.5, 0.25, and 0.125
- $\beta_0 = 0.18$ in higher magnetic field upstream region
- $-7 \leq x \leq 7$, $0 \leq y \leq 30$; conducting wall BCs
- High resolution needed over a larger area
- Caveats:
  - 1-D initial equilibrium with no vertical stratification
  - Single X-line in resistive MHD
  - Neglect 3-D effects
  - Unphysical upper conducting wall BC
  - β larger than reality
- See Murphy et al. (2012, ApJ) for details

Reconnection with both asymmetric inflow and outflow

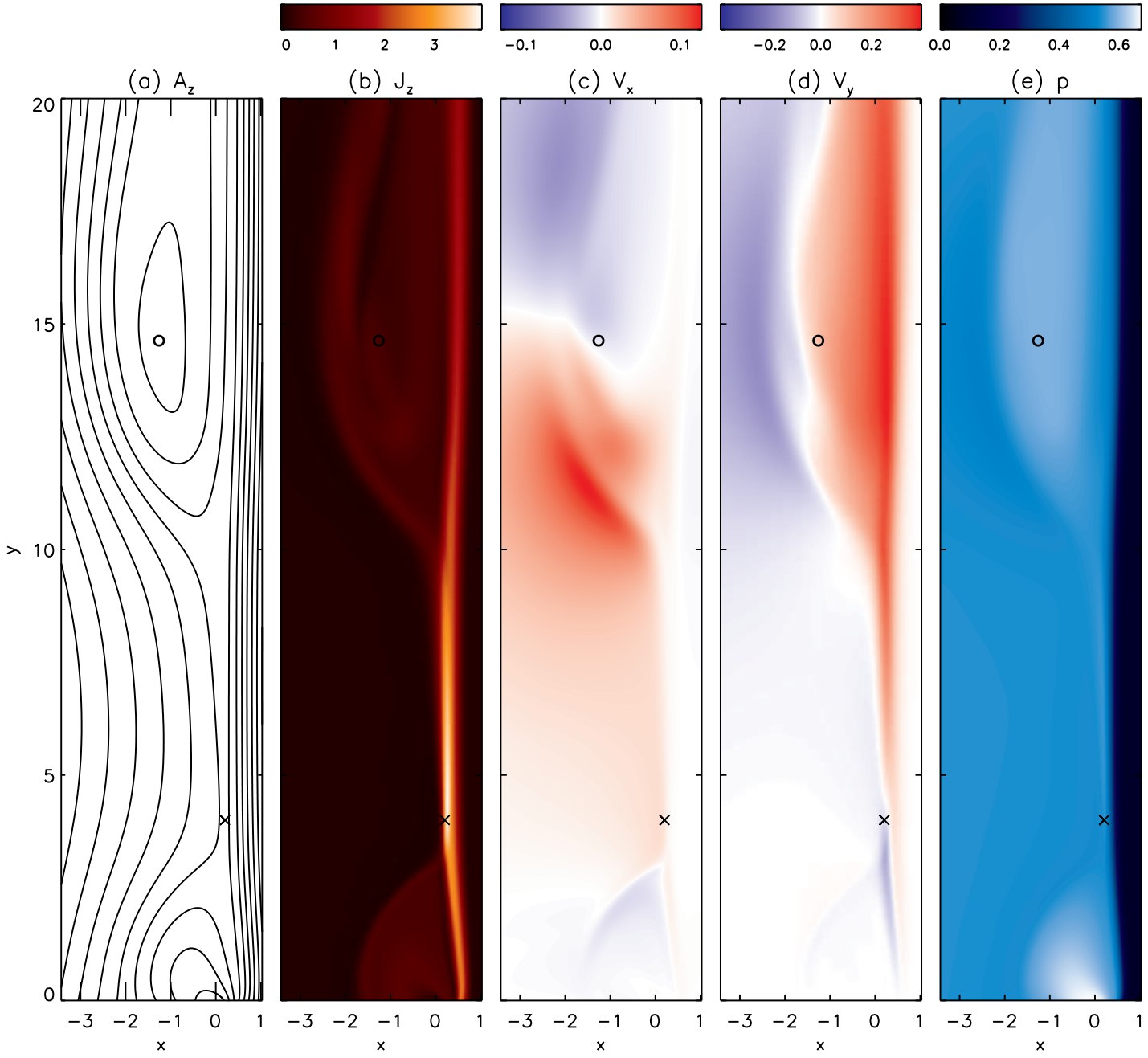

The location of the principal X-line helps determine where released energy goes

- The principal X-line is generally located near the lower base of the current sheet
  - Most of the released energy is directed upward
  - Consistent with numerical and analytical results (Seaton 2008; Reeves et al. 2010; Murphy 2010; Shen et al. 2011)
  - However, during one guide field simulation the X-line drifted to the top of the current sheet
- The X-line usually drifts slowly into the strong field region

There is significant plasma flow across the X-line in both the inflow and outflow directions (see also Murphy 2010)

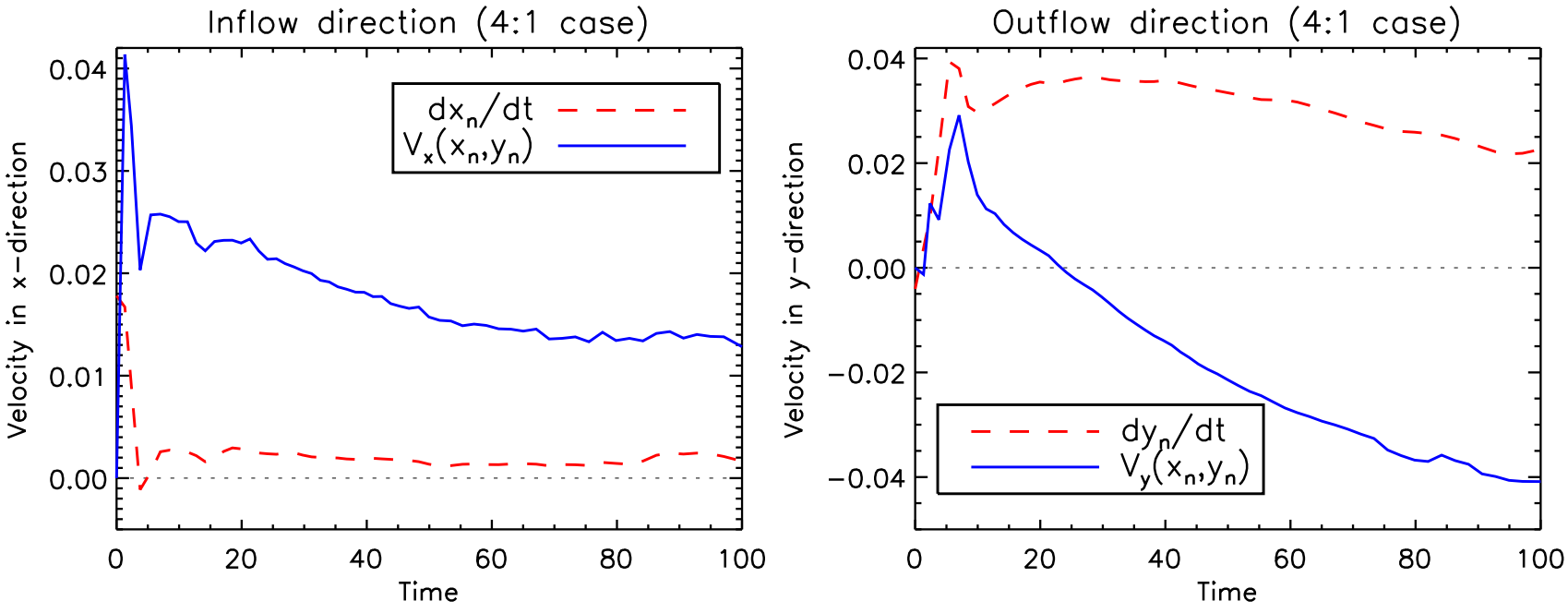

- $V_x(x_n, y_n)$ and $V_y(x_n, y_n)$ give the flow velocity at the X-line
- $\mathrm{d}x_n/\mathrm{d}t$ and $\mathrm{d}y_n/\mathrm{d}t$ give the rate of X-line motion
- X-line motion results from a combination of:
  - Advection by the bulk plasma flow
  - Diffusion of the magnetic field
- No flow stagnation point within the CS in simulation frame

The post-flare loops develop a skewed candle flame shape

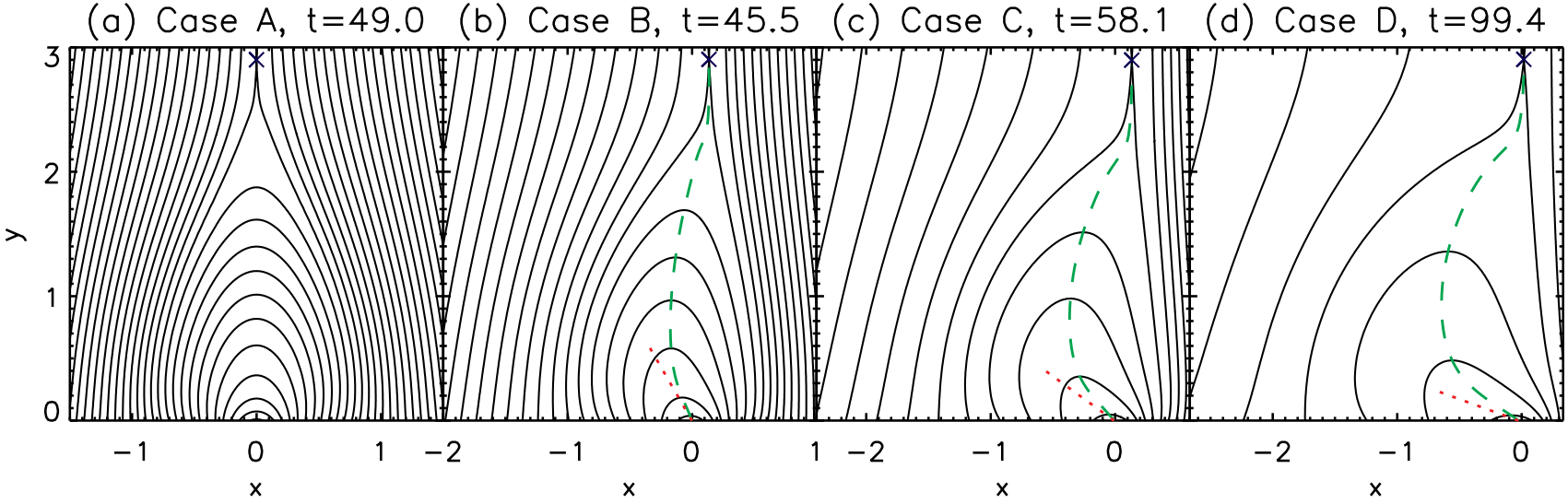

- Magnetic flux contours for $B_L/B_R \in \{1,\ 0.5,\ 0.25,\ 0.125\}$ when $y_n \approx 2.9$
- Dashed green line: loop-top positions
- Dotted red line: analytic asymptotic approximation

The Tsuneta (1996) flare is a famous candidate event

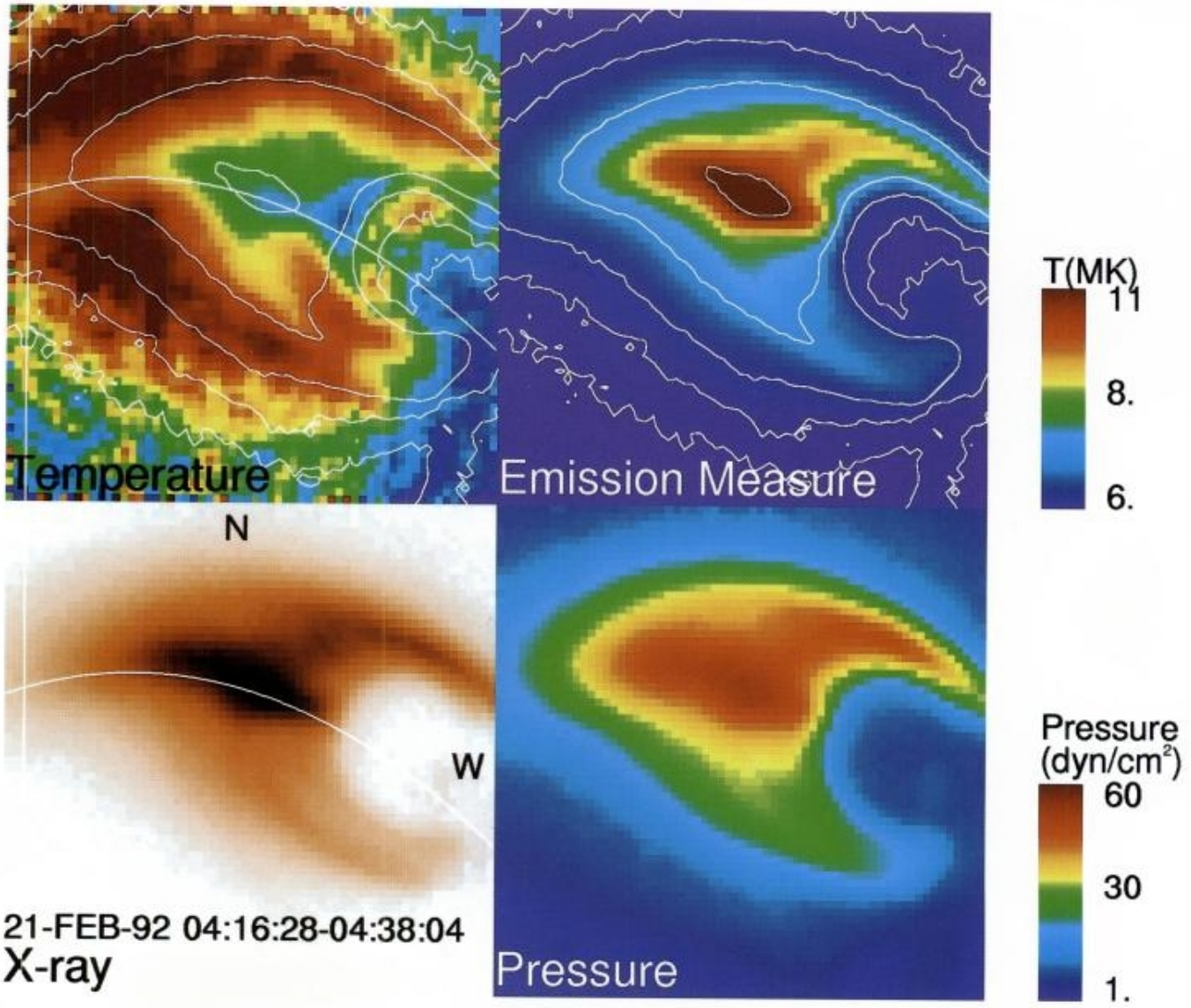

- Shape suggests north is weak **B** side

Fitting simulated asymmetric loops to multi-viewpoint observations constrains the asymmetry

SDO

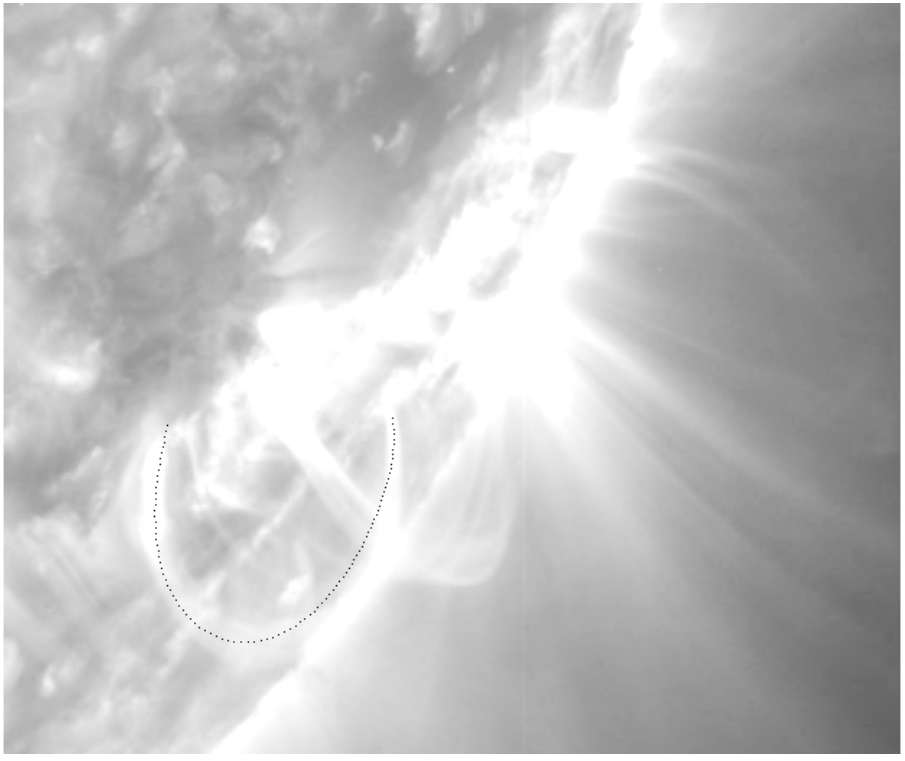

STEREO A

- Most important constraints
  - Location of looptop relative to footpoints
  - Different perspectives from *STEREO A/B* and *SDO*
- Results for two events: asymmetries between 1.5 and 4.0
- Next step: compare to photospheric magnetograms

With D. Ranquist and M. P. Miralles

Asymmetric speeds of footpoint motion

- The footpoints of newly reconnected loops show apparent motion away from each other as more flux is reconnected
- In 2-D, the amount of flux reconnected on each side of the loop must be equal to each other
- The footpoint on the strong **B** side will move slower than the footpoint on the weak **B** side
- Because of the patchy distribution of flux on the photosphere, more complicated motions frequently occur

Asymmetric hard X-ray (HXR) footpoint emission

- The standard model of flares predicts HXR emission at the flare footpoints from energetic particles (EPs) impacting the chromosphere
- Magnetic mirroring reflects energetic particles (EPs) preferentially on the strong **B** side
- More particles should escape on the weak **B** side, leading to greater HXR emission
- This trend is observed in $\sim 2/3$ of events

The outflow plasmoid develops net vorticity because the CS outflow impacts it at an angle

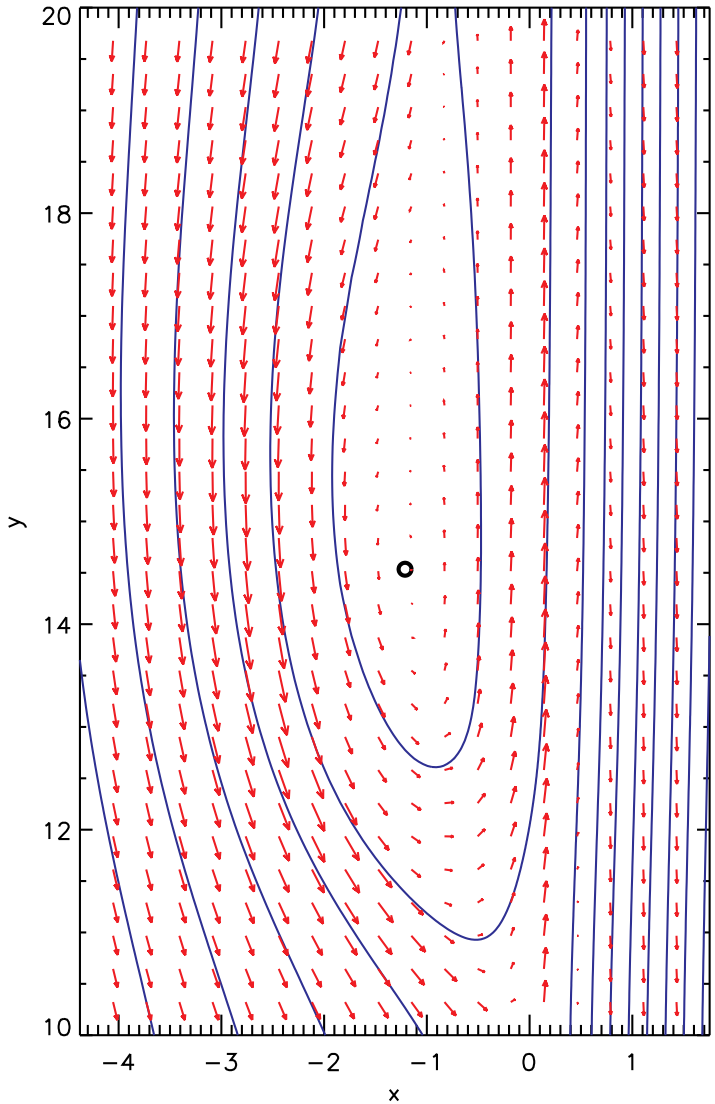

- Velocity vectors in reference frame of O-point

Part II: The plasmoid instability during asymmetric inflow reconnection

NIMROD simulations of asymmetric plasmoid instability

- Reconnecting magnetic fields are asymmetric:

$$B_y(x) = \frac{B_0}{1+b} \tanh\left(\frac{x}{\delta_0} - b\right) \tag{2}$$

- A small number of localized initial magnetic perturbations placed asymmetrically along $z = 0$ near center of domain
- Symmetric case: $\{B_1, B_2\} = \{1, 1\}$; $S_{Ah} \sim 10^5$ $V_{Ah} = 1.0$
- Asymmetric case: $\{B_1, B_2\} = \{0.25\}$; $S_{Ah} \sim 5{\times}10^4$, $V_{Ah} = 0.5$
- Uniform initial density
- $\beta_0 = 1$ in higher magnetic field upstream region
- Domain: $-150 \leq x \leq 150$, $-16 \leq z \leq 16$
- Boundary conditions: periodic along outflow direction and conducting wall along inflow direction
- No mesh packing along outflow direction, and modest resolution requirements in strong **B** upstream region

Numerical considerations

- Mesh packing required over longer stretch along inflow direction
  - X-lines drift toward strong magnetic field upstream region
  - Somewhat less resolution required along outflow direction than in symmetric case
  - Higher resolution required in weak **B** upstream region than in strong **B** upstream region
- Preliminary simulations showed sloshing/oscillatory behavior
  - Symmetric perturbations led to asymmetric magnetic pressure imbalance
  - Resolved by using weak, localized perturbations and increasing the size of the domain along the inflow direction

Plasmoid instability: symmetric inflow

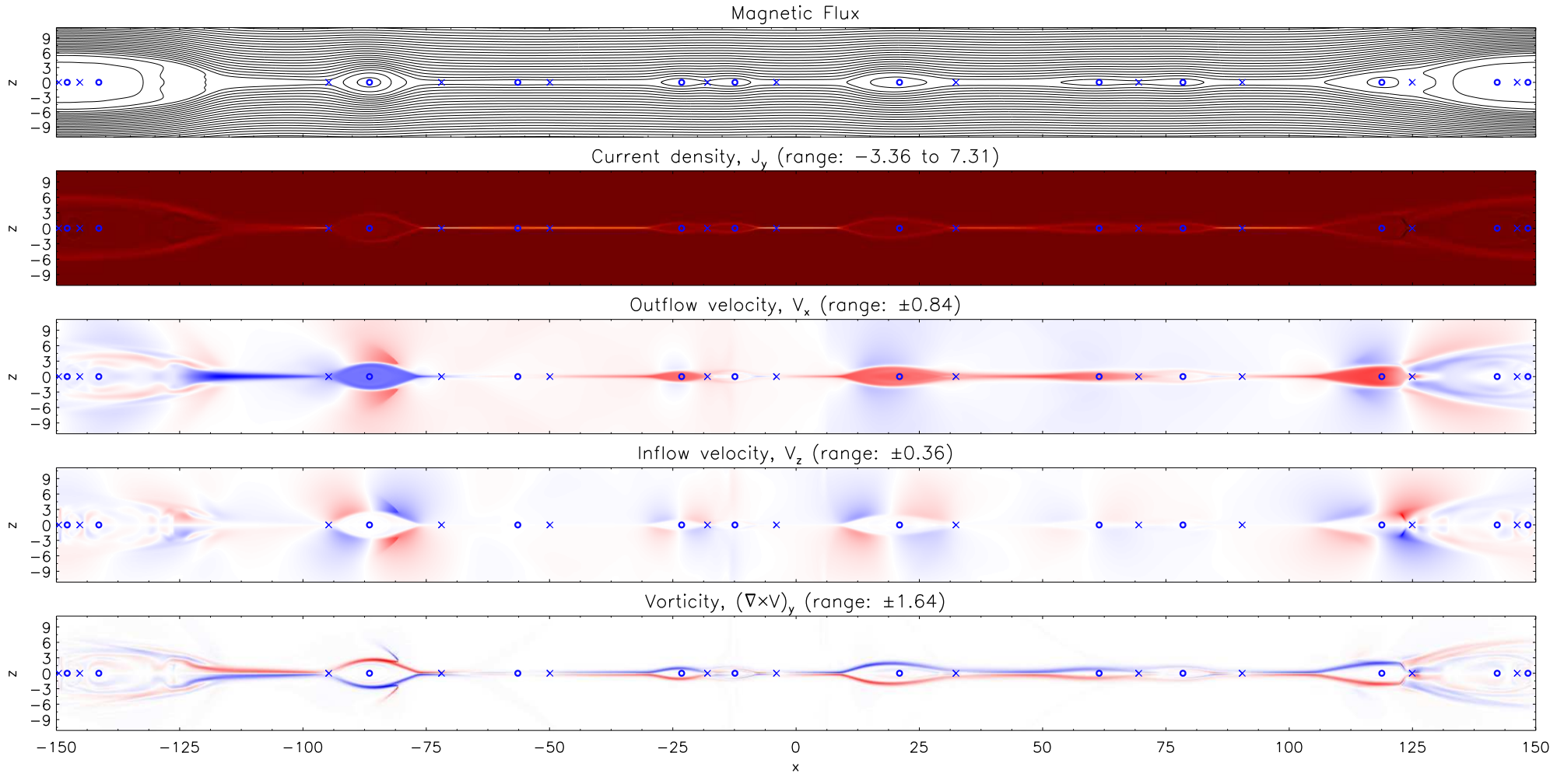

Plasmoid instability: asymmetric inflow

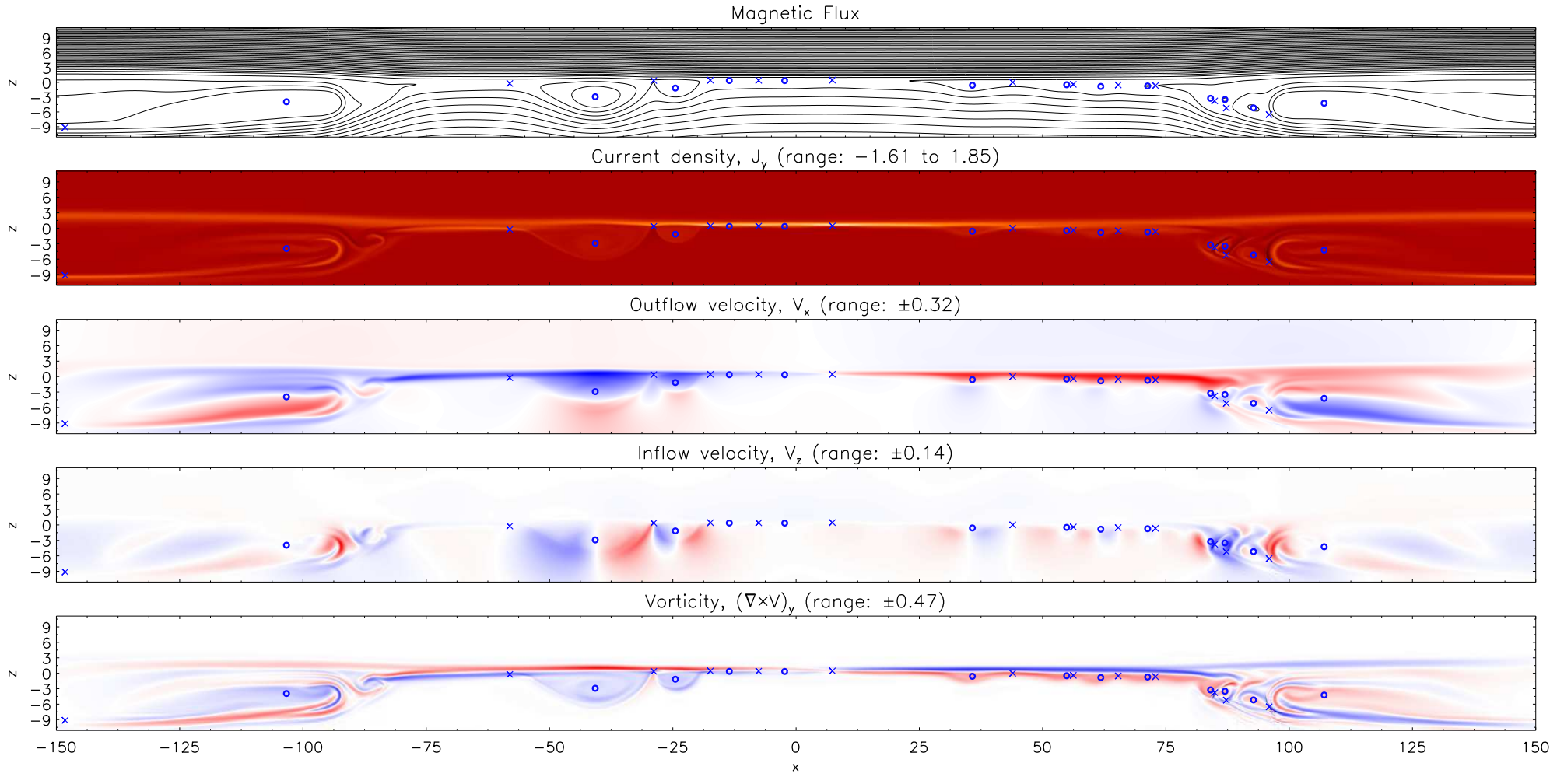

Key features of symmetric inflow simulation

- X-points and O-points all located along $z = 0$
  - Makes it easy to find nulls
- X-lines often located near one exit of each current sheet
  - Characteristic single-wedge shape
- There is net plasma flow across X-lines
  - Flow stagnation points not co-located with X-line
  - The velocity of each X-line differs from the plasma flow velocity at each X-line (see Murphy 2010)
- Outflow jets impact islands directly
  - No net vorticity in islands and downstream regions
  - Less noticeable turbulence in downstream regions
- Outflow velocity $\sim 5/6$ of Alfvén speed

Key features of asymmetric inflow simulation

- Maximum outflow velocity is $\sim 2/3$ of V_{Ah}
- Current sheets thicker than symmetric case
- X-lines vary in position along inflow direction
- Islands develop preferentially into weak **B** upstream region
- Outflow jets impact islands obliquely
  - Islands advected outward less efficiently
  - Net vorticity develops in each magnetic islands
- Downstream region is turbulent
  - Plasmoids impacting and merging with downstream island
  - Several X-points and O-points
- Very little happening in strong **B** upstream region
  - Less resolution needed than in weak **B** upstream region
- Secondary reconnection events (when islands merge) have asymmetric inflow and outflow

The asymmetric case shows little enhancement in the reconnection rate from the predicted value

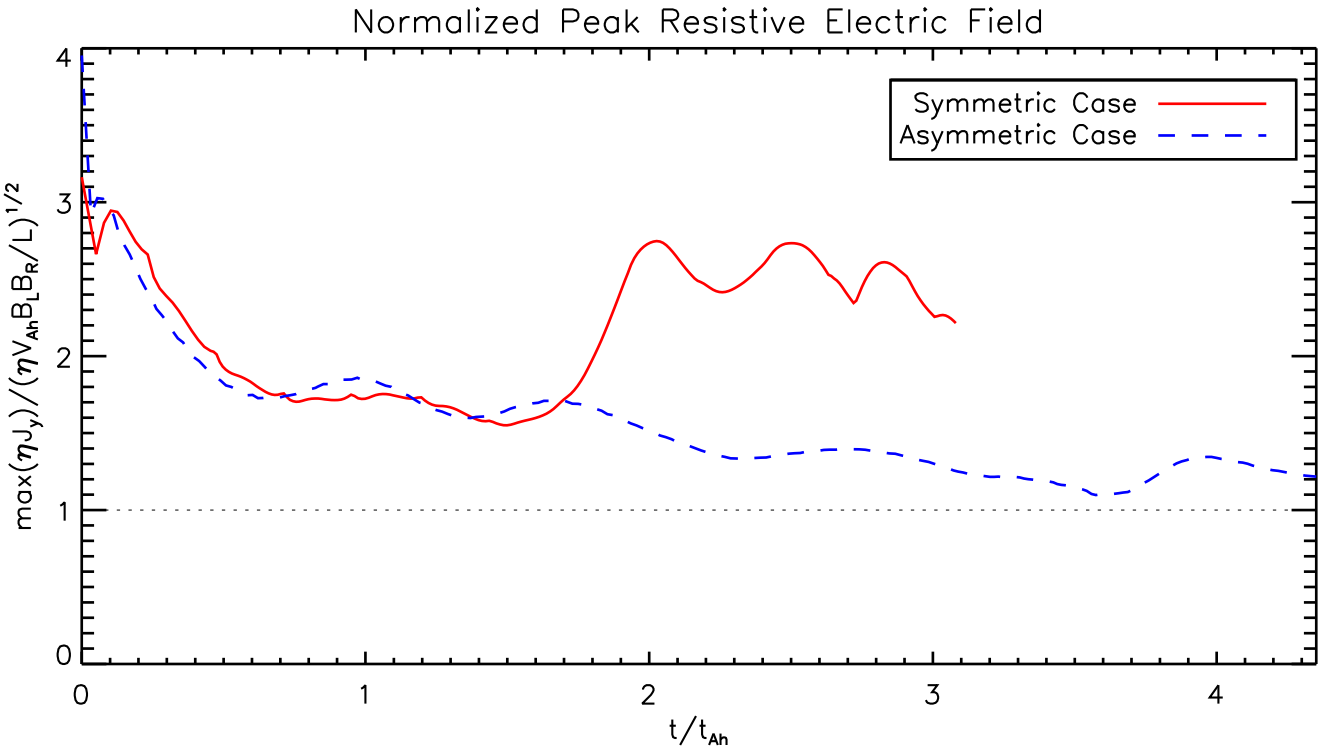

- Use formulae from Cassak & Shay (2007); Birn et al. (2011):

$$E_{predict} = \sqrt{\frac{\eta V_{Ah}}{L} B_L B_R} \qquad t_{Ah} = \frac{L}{V_{Ah}} \qquad L = 100$$

- Note: S_{Ah} is lower by a factor of two for the asymmetric case

On the motion of 3D nulls (with C. Parnell & A. Haynes)

- Murphy (2010) derived an exact expression for the rate of X-line retreat when it is restricted to 1D

$$\frac{\mathrm{d}x_n}{\mathrm{d}t} = \left.\frac{\partial E_y/\partial x}{\partial B_z/\partial x}\right|_{x_n} = V_x\left(x_n\right) - \eta\left[\frac{\frac{\partial^2 B_z}{\partial x^2} + \frac{\partial^2 B_z}{\partial z^2}}{\frac{\partial B_z}{\partial x}}\right]_{x_n} \tag{3}$$

- The 3D equivalent for the motion of isolated magnetic nulls is

$$\frac{\mathrm{d}\mathbf{x}_n}{\mathrm{d}t} = \left(\nabla\mathbf{B}\right)^{-1}\nabla\times\mathbf{E} = \mathbf{V}\left(\mathbf{x}_n\right) - \left[\eta\left(\nabla\mathbf{B}\right)^{-1}\nabla^2\mathbf{B}\right]_{\mathbf{x}_n} \tag{4}$$

- This provides insight into how nulls form, move, and disappear
  - Plasma flow across nulls allowed by resistive diffusion
  - When the Jacobian matrix $\nabla\mathbf{B}$ is singular, nulls are either appearing or disappearing
  - Newly formed null-null pairs initially move apart very quickly
- Allows convenient tracking of nulls in 2D and 3D simulations

Conclusions

- The observational signatures of asymmetric reconnection during solar eruptions include:
  - Skewing/distortion of post-flare loops into a skewed candle flame shape
  - The weak field footpoint moves more quickly and has stronger hard X-ray emission
  - The X-line drifts slowly into the strong field region
  - Net vorticity in the rising flux rope
- Features of the asymmetric plasmoid instability include:
  - X-line positions not all at same location along inflow direction
  - Islands develop into the weak **B** upstream region
  - Outflow jets impact islands obliquely
    - Less efficient outward advection of islands
    - Circulation within each island
  - Turbulence in the downstream region
  - Broader current sheets than the symmetric case
  - The reconnection rate is not greatly enhanced above the predicted value for asymmetric reconnection without plasmoids

Computational Issues

- Simulations are performed using NASA's Pleiades cluster
- Main limitation is memory management for large 2D simulations
  - Running largest jobs on 9 of 12 cores on nodes with 48 GB

Future work with NIMROD (recent NSF/DOE proposal)

- Topics in recent NSF/DOE proposal with J. King and M. Oka
  - Compare dynamics of X-line retreat using two-fluid NIMROD and PIC simulations (with Mitsuo Oka)
  - Plasmoid instability during asymmetric inflow reconnection
  - Scaling behavior of X-line retreat in resistive MHD
    - How do global conditions affect local dynamics of X-line retreat?
  - 3D simulations of two competing reconnection sites
    - Provide insight into
- How do energetic particles affect the reconnection process?
  - Huge fraction of available electrons are accelerated
  - We sorta know how particles are accelerated, but don't know how energetic particles feed back on the reconnection process

Extra slides

What sets the rate of X-line retreat?

- The inflow (z) component of Faraday's law for the 2D symmetric inflow case is

$$\frac{\partial B_z}{\partial t} = -\frac{\partial E_y}{\partial x} \tag{5}$$

- The convective derivative of B_z at the X-line taken at the velocity of X-line retreat, $\mathrm{d}x_n/\mathrm{d}t$, is

$$\left.\frac{\partial B_z}{\partial t}\right|_{x_n} + \frac{\mathrm{d}x_n}{\mathrm{d}t}\left.\frac{\partial B_z}{\partial x}\right|_{x_n} = 0 \tag{6}$$

The RHS of Eq. (6) is zero because $B_z(x_n, z = 0) = 0$ by definition for this geometry.

Deriving an exact expression for the rate of X-line retreat

- From Eqs. 5 and 6:

$$\frac{\mathrm{d}x_n}{\mathrm{d}t} = \left.\frac{\partial E_y/\partial x}{\partial B_z/\partial x}\right|_{x_n} \tag{7}$$

- Using $\mathbf{E} + \mathbf{V} \times \mathbf{B} = \eta \mathbf{J}$, we arrive at

$$\frac{\mathrm{d}x_n}{\mathrm{d}t} = V_x(x_n) - \eta \left[\frac{\frac{\partial^2 B_z}{\partial x^2} + \frac{\partial^2 B_z}{\partial z^2}}{\frac{\partial B_z}{\partial x}}\right]_{x_n} \tag{8}$$

- $\frac{\partial^2 B_z}{\partial z^2} \gg \frac{\partial^2 B_z}{\partial x^2}$, so X-line retreat is caused by diffusion of the normal component of the magnetic field along the inflow direction
- This result can be extended to 3D nulls and to include additional terms in the generalized Ohm's law

The X-line moves in the direction of increasing total reconnection electric field strength

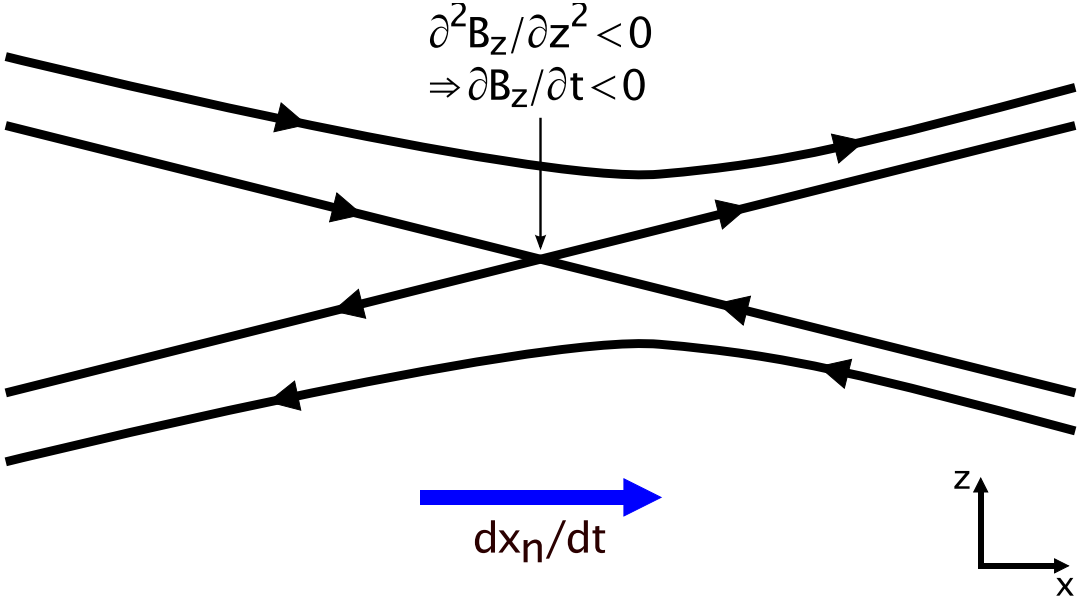

- X-line retreat occurs through a combination of:
  - Advection by the bulk plasma flow
  - Diffusion of the normal component of the magnetic field
- X-line motion depends intrinsically on local parameters evaluated at the X-line
  - X-lines are not (directly) pushed by pressure gradients

Different approaches for studying reconnection

- Laboratory experiments
  - *Advantages*: experimental control, fantastic diagnostic capabilities, simultaneous view of small and large scales
  - *Disadvantages*: modest dimensionless parameters/separation of scales, boundary conditions affecting results
- *In situ* measurements in near-Earth space plasmas
  - *Advantages*: extremely detailed data at a small number of points, great for studying collisionless effects
  - *Disadvantages*: difficult to connect to global dynamics or distinguish between cause and effect
- Solar observations
  - *Advantages*: large-scale dynamics, parameter regimes inaccessible elsewhere, detailed thermal information
  - *Disadvantages*: cannot observe small scales, magnetic field difficult to diagnose